Identification and Characterization of Functional Cation Coordination Sites in Platelet Endothelial Cell Adhesion Molecule-1†

Denise E. Jackson,‡ Rachel O. Loo,§ M. Trudy Holyst,‡ and Peter J. Newman*,‡,||

Blood Research Institute, The Blood Center of Southeastern Wisconsin, Milwaukee, Wisconsin 53226-3548, Departments of Cellular Biology and Pharmacology, The Medical College of Wisconsin, Milwaukee, Wisconsin 53226-3548, and Protein and Carbohydrate Structure Facility, University of Michigan, Ann Arbor, Michigan 48109-0674

Received January 14, 1997; Revised Manuscript Received May 7, 1997⊗

ABSTRACT: We have employed $^{45}CaCl_2$ binding studies, terbium (Tb^{3+}) luminescence spectroscopy, and electrospray mass spectroscopy (ESI-MS) to identify divalent metal binding properties of soluble recombinant human PECAM-1 (srPECAM-1), and to define unique cation binding domains using short, linear peptide sequences from the protein. PECAM-1 was found to directly interact with $^{45}CaCl_2$, binding 2.3 nmol of Ca^{2+}/nmol of srPECAM-1 with a K_d of 1.17 nM. PECAM-1 was found to contain high-affinity cation binding sites involving amino acids Asp_{443}, Asp_{444}, and Glu_{446} of Ig-domain 5 and residues Glu_{487}, Glu_{490}, Asp_{491}, Glu_{538}, Glu_{540}, and Glu_{542} of Ig-domain 6. The PECAM cation binding sites demonstrated broad specificity for all divalent cations, with Mn^{2+} having a higher affinity than Ca^{2+} or Mg^{2+}. Direct binding of Tb^{3+} to these PECAM peptides was confirmed by ESI-MS. Modeling studies predict that the six cation binding residues within Ig-domain 6 are proximal to each other in three-dimensional space, and may form a single cation coordination site. The identification of cation binding sites in PECAM-1 will direct further work in examining its cation-dependent roles in cellular signaling.

Cell−cell interactions are mediated by distinct transmembrane glycoproteins involving members of the integrin, selectin, cadherin, and Ig-superfamily cell adhesion molecule (Ig-CAM)[1] gene families [for reviews, see Springer (1990) and Hynes (1992)]. Members of the immunoglobulin (Ig) gene superfamily of C2 type cell adhesion receptors share a common structural similarity. These proteins have a variable number of extracellular Ig-domains with conserved cysteine residues that form disulfide bonds to stabilize β-strands into an antibody fold (Williams & Barclay, 1988). A number of members of the Ig-superfamily have been shown to participate in both homophilic and heterophilic cell adhesive interactions. Examples include neural cell adhesion molecule (NCAM), neuron−glia cell adhesion molecule (Ng-CAM), and neuron−glia-related cell adhesion molecule (Nr-CAM) (Cunningham *et al*., 1987; Grumet & Edelman, 1988; Mauro *et al*., 1992; Murray *et al.*, 1992; Rao *et al*., 1992).

Platelet endothelial cell adhesion molecule-1 (PECAM-1/CD31) is a 130 kDa member of the Ig-CAM superfamily that is constitutively expressed on vascular endothelium, where it is localized to endothelial cell junctions (Newman & Albelda, 1992; Muller *et al*., 1989). It is also present on the surface of human platelets, neutrophils, monocytes, and various T cell subsets (Newman, 1994; Newman *et al*., 1990; Tanaka *et al*., 1992). PECAM-1 appears to play an important role in vascular biology; in particular, it is an important mediator of leukocyte/endothelial cell interactions that take place during the process of transendothelial migration, and may also be important in endothelial cell−cell interactions, angiogenesis, and the inflammatory response (Muller *et al*., 1993; Vaporician *et al*., 1993; Bogen *et al*., 1994; Albelda *et al*., 1990; Baldwin *et al*., 1994). The mechanisms by which PECAM-1 mediates cellular interactions appear to be complex. Several lines of evidence have suggested a Ca^{2+}-independent homophilic PECAM interaction: COS cells transiently transfected with PECAM-1 cDNA express PECAM-1 at the intracellular junctions of adjacently transfected COS cells, but not at the junctions between transfected and nontransfected cells (Albelda *et al*., 1991). Recombinant PECAM-1 on the surface of 3T3 cells also interacts with native PECAM-1 on human endothelial cells (Albelda *et al*., 1991). PECAM-1 antibodies can disrupt endothelial contact sites and delay the ability of endothelial cells to form a confluent monolayer (Albelda *et al*., 1990; Fawcett *et al*., 1995); however, Ca^{2+} chelation using EGTA does not disrupt PECAM-1-mediated adhesions at the endothelial cell junctions (Ayalon *et al*., 1994). Finally, phospholipid vesicles expressing purified human platelet PECAM-1 and a human PECAM chimera-IgG bind specifically to cells expressing PECAM-1 in a Ca^{2+}-independent manner (Sun, Q.-H., *et al*., 1996). This homophilic PECAM interaction is mediated by

† This investigation was supported by Grant HL-40926 (to P.J.N.) from the National Institutes of Health. D.E.J. is a recipient of an American Heart Association Postdoctoral Award (96F-Post-34) (Wisconsin Affiliate). P.J.N. is an Established Investigator (92001390) of the American Heart Association.

* Address correspondence to this author at the Blood Research Institute, The Blood Center of Southeastern Wisconsin, 638 N. 18th St., Milwaukee, WI 53233-2194. Phone: (414) 937-6284. Fax: (414) 937-6284.

‡ The Blood Center of Southeastern Wisconsin.

§ University of Michigan.

|| The Medical College of Wisconsin.

⊗ Abstract published in *Advance ACS Abstracts,* July 15, 1997.

[1] Abbreviations: Ig-CAM, immunoglobulin superfamily cell adhesion molecule; NCAM, neural cell adhesion molecule; Ng-CAM, neuron−glia cell adhesion molecule; Nr-CAM, neuron−glia-related cell adhesion molecule; GAGS, glycosaminoglycans; LAK, lymphokine activated killer; ESI-MS, electrospray mass spectroscopy; *m/z*, mass/charge ratio; MIDAS, metal ion dependent adhesion site; srPECAM-1, soluble recombinant PECAM-1.

S0006-2960(97)00084-6 CCC: $14.00

Ig-homology domains 1 and 2 (Sun, Q.-H., *et al*., 1996; Sun, J., *et al*., 1996).

PECAM-1 has also been implicated in heterophilic cell interactions, as demonstrated by the Ca^{2+}-dependent interactions of PECAM-1-transfected mouse L-cells with nontransfected L-cells. This interaction can be blocked by anti-PECAM antibodies which map to Ig-domains 2 and 6 (Albelda *et al*., 1991; Yan *et al*., 1994), cell surface glycosaminoglycans (GAGS), and the hexapeptide sequence, LKREKN, present in Ig-domain 2 that is partially homologous to a heparin binding consensus sequence (DeLisser *et al*., 1993; Albelda *et al*., 1992). The requirement for divalent cations in the aggregation of PECAM-1-transfected L-cells has remained unexplained. It is not clear whether this divalent cation dependency is related to PECAM-1 itself, or is contributed by other receptors involved in cellular interactions with PECAM-1. Two recent studies have suggested a role for divalent cation-dependent association of PECAM-1 with an integrin counterreceptor, $\alpha_v\beta_3$ (Piali *et al*., 1995; Buckley *et al*., 1996). Recent experimental evidence has implicated a role for PECAM-1 as an agonist receptor in signal transduction pathways that requires integrin-mediated cell−cell contact as a secondary adhesion event (Sun, Q.-H., *et al*., 1996; Jackson *et al*., 1997).

In this study, we have examined the divalent metal binding properties of srPECAM-1 and defined specific cation binding regions in PECAM-1 using synthetic PECAM peptides. We demonstrate that PECAM-1 contains high-affinity cation coordination sites within Ig-domains 5 and 6. These results may assist our understanding of the effects of metal ions on the conformation of PECAM-1 necessary for it to mediate secondary adhesive events mediated by non-PECAM-1 receptors.

EXPERIMENTAL PROCEDURES

Materials. EDTA, pure $CaCl_2$, $MgCl_2$, $MnCl_2$, CHAPS, MOPS, and bovine serum albumin were obtained from Sigma Chemical Co., St. Louis, MO. Chelex-100 was obtained from Bio-Rad Laboratories (Richmond, CA). High-purity terbium chloride was obtained from Aldrich Chemicals (Milwaukee, WI). srPECAM-1 and a recombinant GPIIb fragment encompassing amino acids 174−449 were prepared as previously described (Goldberger *et al*., 1994; Jackson *et al*., 1996). Each protein was shown to be >95% pure on a Coomassie Blue stained SDS−PAGE gel. For experiments requiring metal-free conditions, proteins were extensively dialyzed at 4 °C for 24 h in Chelex-treated 50 mM MOPS, pH 6.5, containing 0.1% CHAPS.

Peptide Synthesis. PECAM peptides were synthesized using a Model 9050 Pepsynthesizer (Millipore, Bedford, MA) with 9-fluoronylmethoxycarbonyl (FMOC) chemistry according to standard manufacturer's instructions. Peptides were deblocked using 25% piperidine. Amino acids were introduced as preformed active esters and activated with 0.3 M 1-hydroxybenzotriazole hydrate in dimethylacetamide. The peptides were then cleaved from the resin using a mixture of 87.5% trifluoroacetic acid/5% thioanisole/2.5% ethanethiol/5% H_2O, precipitated with ether, washed extensively with cold ether, dried under nitrogen, dissolved in distilled water, and dried by lyophilization (Aldrich Chemicals, Milwaukee, WI). Peptides were then purified by reversed-phase HPLC (Beckman Instruments, San Ramon, CA) to >85% purity on a C_{18} column (Vydac, Hesperia, CA) using an aqueous trifluoroacetic acid (0.1%)/acetonitrile-based mobile phase. All purified peptides were analyzed by fast atom bombardment mass spectroscopy (Mass Spectroscopy Laboratory, Medical College of Wisconsin, Milwaukee, WI) to confirm the expected molecular mass.

Fluorescence Energy Transfer Spectroscopy. Tb^{3+} luminescence measurements of PECAM peptides and srPECAM-1 were performed using an SLM MC400 monochromator spectrofluorometer (SLM-Aminco, Urbana, IL) equipped with an on-line IBM computer running 8100 spectrofluorometer software, and connected to an RTE-210 NESLAB refrigerated waterbath at 20 °C. Emission spectra were taken with excitation and emission band-passes of 2 nm and 4 nm, respectively. The excitation wavelength was chosen at 290 nm with a Tb^{3+} emission at 545 nm. All samples were diluted in 50 mM MOPS, pH 6.5, containing 0.1% CHAPS, which had been pretreated with Chelex-100 and analyzed within 4 h after the addition of Tb^{3+}. In these experiments, titrations were performed with a constant amount of 50 μM Tb^{3+} solution and increasing concentrations of PECAM peptides or, alternatively, a constant amount of 25 μM peptide solution with increasing concentrations of Tb^{3+} solution. Results are expressed as luminescence [F(total) − F_o(background without peptide)] expressed in arbitrary units versus Peptide:Tb^{3+} ratio. The red-shifted harmonic at 580 nm was monitored on all spectroscopic scans to ensure that the peptide−terbium complexes remained in solution, and that no peptide or protein aggregates had formed during the incubation. Levels of Ca^{2+} in buffers and protein samples were determined using a calcium Model 93-20 electrode according to the manufacturer's instructions (Orion Research Inc., Boston, MA). Specificity of divalent cation binding was confirmed by displacement of Tb^{3+} by Ca^{2+}, Mg^{2+}, and Mn^{2+} ions. The sequential reduction in emission intensity at 545 nm was measured after addition of 10 μL aliquots of 50 mM $CaCl_2$, $MgCl_2$, or $MnCl_2$. Binding constants were determined from these competition experiments for the interaction of each divalent cation with each candidate PECAM peptide using the following equation: $K_a = \upsilon/\{(1 - \upsilon)(R - \upsilon)[P]\}$, where R = ratio of $[\text{divalent cation}]_{tot}/[Tb^{3+}]_{tot}$ at which a 50% reduction in fluoresence intensity was obtained; and $\upsilon = F_{50\%}/F_{tot}$, where υ is the relative change in fluorescence intensity at a given wavelength. $[Tb^{3+}]_{tot}$, $[\text{divalent cation}]_{tot}$, and [P] are the final concentrations of Tb^{3+}, competing divalent cation, and PECAM peptide used in the assay (Borin *et al*., 1989).

Modifications of PECAM-1 Peptides for Fluorescence Energy Transfer Spectroscopy. For convenience, amino acid substitutions are numbered according to their respective position in the peptide sequence. The sequence of the PECAM 534−549 loop 6 peptide was modified by the placement of a Trp residue instead of a Tyr residue at position 11, while PECAM 485−495 loop 6 peptide sequence was modified by placement of a Tyr residue instead of a Val residue at position 2 and a Trp residue instead of a Leu residue at position 10. The PECAM 436−448 loop 5 peptide was modified by placement of a Tyr residue at position 2 instead of a Phe residue and a Trp residue at position 12 instead of a Tyr residue. For the two Ig-domain 2 peptides, PECAM 164−178 was modified by placement of a Tyr residue at position 3 instead of a Phe residue and a Trp residue at position 14 instead of a Phe residue. The sequence

of PECAM 135−148 peptide was modified by placement of a Tyr residue in position 2 instead of a Phe residue and a Trp residue at position 14 instead of a Val residue.

Circular dichroism (CD) measurements were performed on a JASCO Model J-710 spectropolarimeter fitted with a thermally regulated cell holder in 1 mm rectangular quartz cuvettes. The native and modified PECAM (Y,W) peptides (0.2 mg/mL) were dissolved in 17% acetonitrile/H_2O and analyzed by CD spectra analysis from 260 to 195 nm, every 0.5 nm, with 2 s collection times. CD spectra for the Y,W-substituted peptides showed slight differences from those of the native peptides. More negative values of ellipticity were observed for 436Y,W relative to 436 and for 534W relative to 534 from 195−220 nm, but especially in the 195−200 nm range, consistent with increased random-coil contributions to the structures of the substituted peptides. Less negative values of ellipticity were observed for 485Y,W relative to 485 from 195 to 250 nm. To confirm that these differences did not affect the cation binding properties of the modified PECAM (Y,W) peptides, we compared direct binding of Tb^{3+} to both native and modified PECAM (Y,W) peptides by ESI-MS and found them to be identical.

Competition Inhibition Assay. srPECAM-1 was evaluated for its ability to bind divalent cations using a competition inhibition assay (Jackson *et al*., 1996). Briefly, a 14 amino acid peptide comprising the first calcium binding domain of platelet membrane glycoprotein (GP) IIb (GPIIb 242−255) was used as a reporter peptide at a fixed concentration of 20 μM in the presence of 50 μM Tb^{3+}. The peptide/Tb^{3+} mixture was excited at 290 nm, and the luminescence resulting from energy transfer to bound Tb^{3+} was recorded at 545 nm. Addition of metal binding proteins in increasing nanomolar concentrations to the reporter peptide/Tb^{3+} mixture results in a dose-dependent decrease in Tb^{3+} luminescence. All results are expressed as percent inhibition versus competitor concentration.

Electrospray Mass Spectroscopy (ESI-MS). Candidate PECAM-1 and control peptides (50 μM) were dissolved in distilled water and incubated overnight at 4 °C in the presence or absence of 25 μM $TbCl_3$. Samples were dried using a Speedvac SC100 evaporator (Savant Instruments, Farmingdale, NY). Peptide samples with and without $TbCl_3$ were rehydrated in 100% Millipore water and analyzed immediately to minimize dimer formation. Samples were delivered by continuous infusion at 5 μL/min to a Vestec 201 quadrupole mass spectrometer (2000 *m/z* range). The Vestec electrospray ionization source did not require liquid sheath flow, SF_6, or nebulizing gas to spray 100% aqueous solutions (Protein and Carbohydrate Structure Facility, University of Michigan, Ann Arbor, MI).

Equilibrium Dialysis of $^{45}CaCl_2$. $^{45}CaCl_2$ binding studies were performed using 8-well dialysis modules (EMD101B multi-sample microvolume dialyzer, MW cutoff 12 000−14 000, 0.25 mL cell, Hoefer Scientific Instruments). A 0.25 mL aliquot of srPECAM-1 (0.65 mg/mL) in Chelex-treated 0.01 M PBS, pH 7.4, was placed in one side of the dialysis membrane in chamber 1, while an equal volume of Chelex-treated 0.01 M PBS, pH 7.4, containing various amounts of $^{45}CaCl_2$ (Amersham, England) was added to the other side of the dialysis membrane in chamber 2. Equilibrium dialysis was performed for 24 h at room temperature. Following incubation, 20 μL aliquots in duplicate were removed from each chamber and transferred into 5 mL of Aquasol.

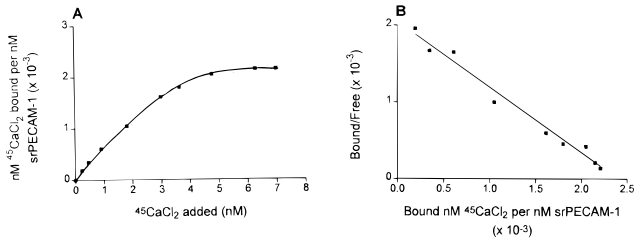

FIGURE 1: Direct Ca^{2+} binding to srPECAM-1. (A) Equilibrium dialysis experiments were performed with $^{45}CaCl_2$ as described under Experimental Procedures. Data presented are representative of six independent experiments. Each point is an average of duplicate measurements. (B) Scatchard plot of the data generated by linear least-squares regression analysis ($y = -0.8579x + 2.045$, $R^2 = 0.9808$).

Radioactivity was quantified in a Pharmacia Wallac 1410 liquid scintillation counter. Data were analyzed using Graph Pad Prism Version 2.0 and Microsoft Excel Version 5.0 to generate binding curves and Scatchard plots using least-squares linear regression analysis.

Computer-Generated β-Sheet Analysis. β-Sheet analysis of PECAM-1's structure was obtained using PC/Gene release 6.70: the nucleic acid and protein sequence analysis software system. Protein secondary structure analysis was performed using the Novotny program (Novotny *et al*., 1984; Rose *et al*., 1980).

RESULTS

Ca^{2+} Binding to srPECAM-1. To determine if srPECAM-1 could directly interact with Ca^{2+}, we measured the binding of $^{45}CaCl_2$ to srPECAM-1 using equilibrium dialysis. In these experiments, srPECAM-1 was dialyzed against increasing concentrations of $^{45}CaCl_2$ (0−7 nM) as described under Experimental Procedures. As shown in Figure 1, srPECAM-1 directly binds $^{45}Ca^{2+}$ with 2.3 nmol of Ca^{2+}/nmol of srPECAM-1 with a K_d of 1.17 nM. In contrast, parallel experiments using albumin as a non-calcium binding protein showed no ability to bind $^{45}Ca^{2+}$ (data not shown).

Divalent Metal Binding Properties of srPECAM-1. The binding of divalent cations to srPECAM-1 may play an important role in maintaining the proper conformation and/or orientation of PECAM-1 necessary for it to mediate its adhesive interactions. To show further evidence for a divalent cation interaction with PECAM-1, we compared the metal ion binding properties of srPECAM-1 with a recombinant GPIIb polypeptide encompassing all four calcium binding domains using quantitative Tb^{3+} luminescence spectroscopy. Tb^{3+} can substitute for Ca^{2+} with higher affinity in functional ligand binding interactions of metal ion binding proteins (Cierniewski *et al*., 1994). Since some metal binding proteins lack the required aromatic donor residues (Trp, Tyr) in close proximity to cation binding regions necessary to directly detect bound Tb^{3+}, we recently developed a competition assay in which a metal binding protein is used as an inhibitor of Tb^{3+} binding to a reporter peptide that had been optimized for maximal energy transfer (Jackson *et al*., 1996). As shown in Figure 2, when used as a competitive inhibitor, srPECAM-1 could compete for Tb^{3+} ions in a dose-dependent manner, and was nearly as effective as a recombinant GPIIb 174−449 polypeptide that contains four well-characterized calcium binding domains (Jackson *et al*., 1996). For example, at a concentration of 240 nM (10 μg/mL), the rGPIIb polypeptide inhibited Tb^{3+} lumi-

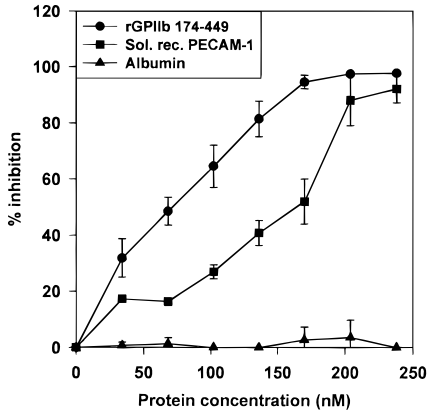

FIGURE 2: Divalent metal binding properties of srPECAM-1 demonstrated by Tb^{3+} binding. srPECAM-1, recombinant GPIIb fragment residues 174−449 (encompassing four well-characterized calcium binding domains), and albumin were each examined for their ability to compete for Tb^{3+} binding to a reporter peptide comprising the first Ca^{2+} binding domain of GPIIb. Results are expressed as the mean ± standard deviation of three independent experiments. Note that srPECAM-1 competes for Tb^{3+} binding, and is nearly as effective as the recombinant GPIIb polypeptide. Albumin, on the other hand, shows no ability to bind divalent cations.

nescence by greater than 95%, while srPECAM-1 achieved 90% inhibition. This could not be attributed to insolubility or aggregation of srPECAM-1 protein, as the harmonic at 580 nm remained constant throughout the assay. Albumin was included as a non-calcium binding protein, and displayed no ability to compete for Tb^{3+} binding. Taken together, these data indicate that PECAM-1 contains functional metal ion binding properties that can modulate the conformation of the protein.

Synthesis and Optimization of Five Candidate Cation Binding Regions in PECAM-1 for Luminescence Spectroscopy. The precise location of cation binding regions within the extracellular Ig-domains of PECAM-1 is not known. Examination of the primary amino acid sequence of PECAM-1 revealed specific regions in Ig-domains 2, 5, and 6 rich in Asp and Glu residues. Peptides corresponding to these candidate cation binding regions in PECAM-1, as well as scrambled versions of these peptides, were synthesized and optimized for Tb^{3+} luminescence energy transfer by appropriate placement of aromatic Trp or Tyr residues as shown in Table 1. The validity of these substitutions was

Table 1: Synthetic PECAM Peptides

Ig Domains 5 and 6 PECAM peptides	
PECAM 436-448	V F K **D N** P T **E D** V **E** Y Q
PECAM 436-448(*Y,W*)	V *Y* K **D N** P T **E D** V **E** *W* Q
PECAM 436-448(*Y,W*) (scrambled)	**E** K P *Y* **D N** T **E** Q V **D** V *W*
PECAM 485-495	V V **E** S G **E D** I V L Q
PECAM 485-495 (*Y,W*)	V *Y* **E** S G **E D** I V *W* Q
PECAM 485-495 (*Y,W*) (scrambled)	**E** *Y* Q S **E** V G I V **D** *W*
PECAM 534-549	K A S K **E** Q **E** G **E** Y Y C T A F **N**
PECAM 534-549 (*W*)	K A S K **E** Q **E** G **E** Y *W* C T A F **N**
PECAM 534-549 (*W*) (scrambled)	S A **E** K Q G T A C Y *W* **E** K F **N E**
Ig Domain 2 PECAM peptides	
PECAM 135-148	H F T I **E** K L **E** L **N E** K M V
PECAM 135-148 (*Y,W*)	H *Y* T I **E** K L **E** L **N E** K M *W*
PECAM 135-148 (*Y,W*) (scrambled)	**E** M **E** *Y* K I T **N** K L **E** H *W* L
PECAM 164-178	L **E** F P V **E E** Q **D** R V L S F R
PECAM 164-178 (*Y,W*)	L **E** *Y* P V **E E** Q **D** R V L S *W* R
PECAM 164-178 (*Y,W*) (scrambled)	P **E** R *Y* V S **E** R L *W* L Q **D** L **E**

established by the following criteria: (1) The amino acids at these positions would not contribute hydrogen bonds to a cation coordination site to stabilize the configuration of the peptide. (2) In most cases, direct substitutions of aromatic amino acids were made to maximize energy transfer. For this purpose, the preferred aromatic amino acids in descending order are Trp, Tyr and Phe residues. (3) CD spectral analysis revealed that the modified PECAM-1 (Y,W) peptides assumed a relatively similar conformation compared to the native PECAM-1 peptides (for details, see Experimental Procedures). (4) Direct Tb^{3+} binding to both native and modified PECAM peptides was virtually identical, as determined by ESI-MS (data not shown). As shown in Figure 3, whereas native candidate cation binding PECAM peptides exhibited weak Tb^{3+} luminescence, the modified candidate PECAM peptides containing the substituted aromatic amino acids, Trp (W) and Tyr (Y), showed significant

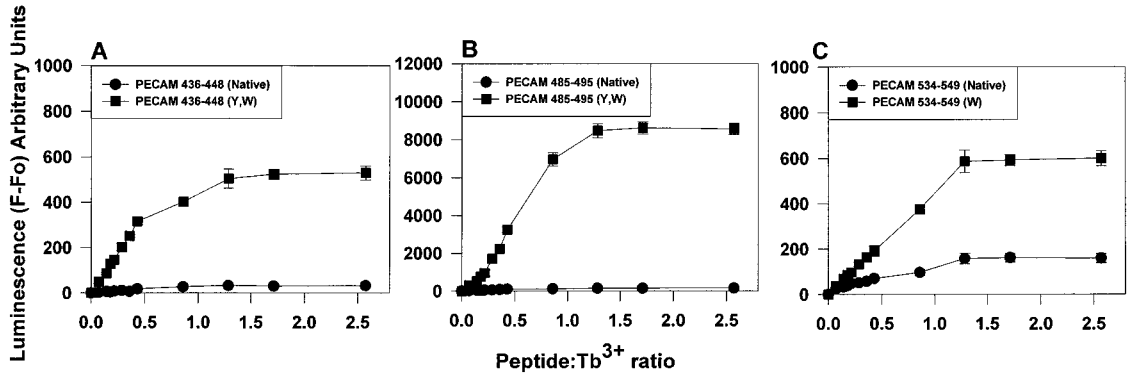

FIGURE 3: Optimization of PECAM-1 Ig-domain 5 and 6 peptides for Tb^{3+} luminescence spectroscopy. Titration curves of the interaction of Tb^{3+} with synthetic peptides encompassing unique regions in PECAM Ig-domains 5 (A) and 6 (B, C). The sequences of the three peptides examined are provided in detail in Table 1, and include the native candidate PECAM sequence (●) and modified candidate PECAM peptides with appropriate placement of aromatic amino acids, Trp and Tyr (■). Results are expressed as the mean ± standard deviation of three independent experiments. Note that the modified peptides exhibited a greatly increased capacity to transfer energy to bound Tb^{3+} compared with native peptides.

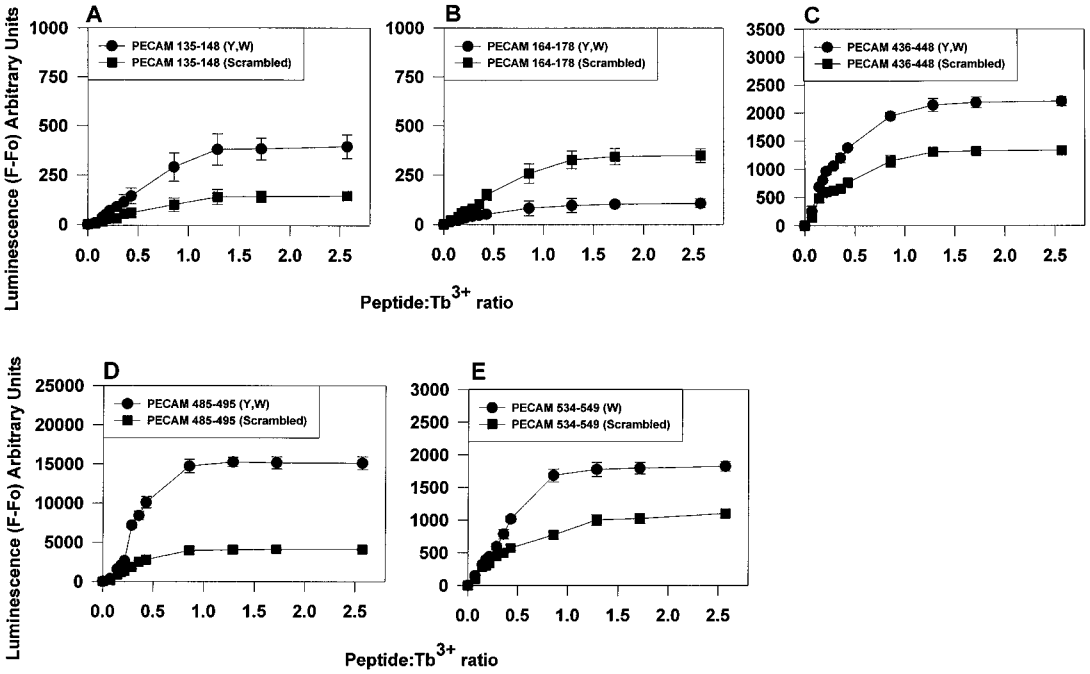

FIGURE 4: Metal binding properties of candidate PECAM Ig-domain 2, 5, and 6 peptides. Titration curves of the interaction of Tb^{3+} with synthetic peptides of candidate sequences in PECAM Ig-domains 2 (A, B), 5 (C), and 6 (D, E). The sequences of the five peptides examined are provided in detail in Table 1, and in each case include a modified wild-type PECAM sequence (Y,W) (●) and a scrambled version of each peptide (■). Results are expressed as the mean ± standard deviation of three independent experiments. Tb^{3+} luminescence was excited at 285 nm and measured at 545 nm. Note that the Ig-domain 5 and 6 peptides showed greatly enhanced luminescence compared to Ig-domain 2 peptides.

Tb^{3+} luminescence at 545 nm upon titration with peptide or $TbCl_3$. Based upon these results, we used the (Y,W) modified peptides in all subsequent experiments.

Metal Binding Properties of PECAM Ig-Domain 2, 5, and 6 Peptides. To examine the metal binding properties of candidate PECAM Ig-domain 2, 5, and 6 (Y,W) peptides, we performed titrations of each peptide with a fixed concentration of $TbCl_3$ or vice versa, and monitored cation binding using Tb^{3+} luminescence spectroscopy. The validity of this approach has been verified by previous studies demonstrating that the conformations of the synthetic peptide loops in solution with Tb^{3+} fold the peptide into the same three-dimensional structure that exists in the intact protein (Gariepy *et al*., 1985; Marsden *et al*., 1989). As shown in Figure 4, when increasing amounts of each candidate PECAM peptide corresponding to Ig-domains 2 (panels A and B), 5 (panel C), and 6 (panels D and E) were added to a solution containing a constant amount of Tb^{3+}, luminescence increased in a dose-dependent manner, indicating that these peptides are capable of binding metal ions. With each peptide, saturation of peptide/Tb^{3+} binding was reached at a (1.0−1.25)/1.0 molar ratio of peptide to Tb^{3+}. The Ig-domain 5 and 6 (Y,W) peptides (436−448, 485−495, and 534−549) showed greatly enhanced Tb^{3+} luminescence, while scrambled versions of these peptides containing the same charged residues were much less effective in transferring energy to Tb^{3+}, demonstrating sequence specificity. In contrast, the Ig-domain 2 (Y,W) peptides (135−148, 164−178) bound Tb^{3+} with much less efficiency (Figure 4A,B). In fact, the PECAM 164−178 Ig-domain 2 (Y,W) peptide showed slightly reduced terbium luminescence relative to that of the scrambled sequence (Figure 4B). The data suggest that the acidic amino acids in Ig-domains 5 and 6 comprise cation binding sites, while those present in Ig-domain 2 should not be considered as potential cation binding sites.

Table 2: Binding Constants of Synthetic PECAM-1 Peptides with Cations[a]

peptide	PECAM Ig-domain	affinity constants (K_a) ($M^{-1} \times 10^4$) Ca^{2+}	Mg^{2+}	Mn^{2+}
PECAM 135−148	2	1.5	1.5	2.6
PECAM 164−178	2	1.4	1.4	2.3
PECAM 436−448	5	3.9	3.8	7.6
PECAM 485−495	6	10.9	10.0	18.7
PECAM 534−549	6	3.7	3.0	5.3

[a] Data represent mean value from three separate experiments. Standard deviations were less than 10%.

In order to demonstrate the specificity of the interaction of Tb^{3+} with these peptides, we conducted displacement studies using various divalent cations. As shown in Figure 5, sequential addition of Ca^{2+}, Mg^{2+}, and Mn^{2+} ions resulted in displacement of prebound Tb^{3+} from the candidate PECAM Ig-domain 2 (panels A and B), 5 (panel C), and 6 (panels D and E) (Y,W) peptide sequences, as demonstrated by a dose-dependent reduction in Tb^{3+} luminescence. To displace 50% of the receptor bound Tb^{3+}, a 60−70-fold molar excess of Ca^{2+} or Mg^{2+} ions or a 30−40-fold molar excess of Mn^{2+} ions was required. From these competition studies, we derived binding constants for the interaction of each divalent cation with each region of the PECAM-1 molecule. As shown in Table 2, Ig-domain 2 peptides have relatively low affinity for divalent cations, as predicted by their relatively weak Tb^{3+} luminescence (Figure 4A,B). However, the Ig-domain 5 peptide and both Ig-domain 6 peptides exhibited a 3−5-fold higher affinity for each of the divalent cations compared to the Ig-domain 2 peptides (for example, affinity constants for competing Ca^{2+} ion indicated that the PECAM 485−495 Ig-domain 6 peptide showed a K_a value of 10.9×10^4 M^{-1} compared to 1.4×10^4 M^{-1} for the PECAM 164−178 Ig-domain 2 peptide). These binding

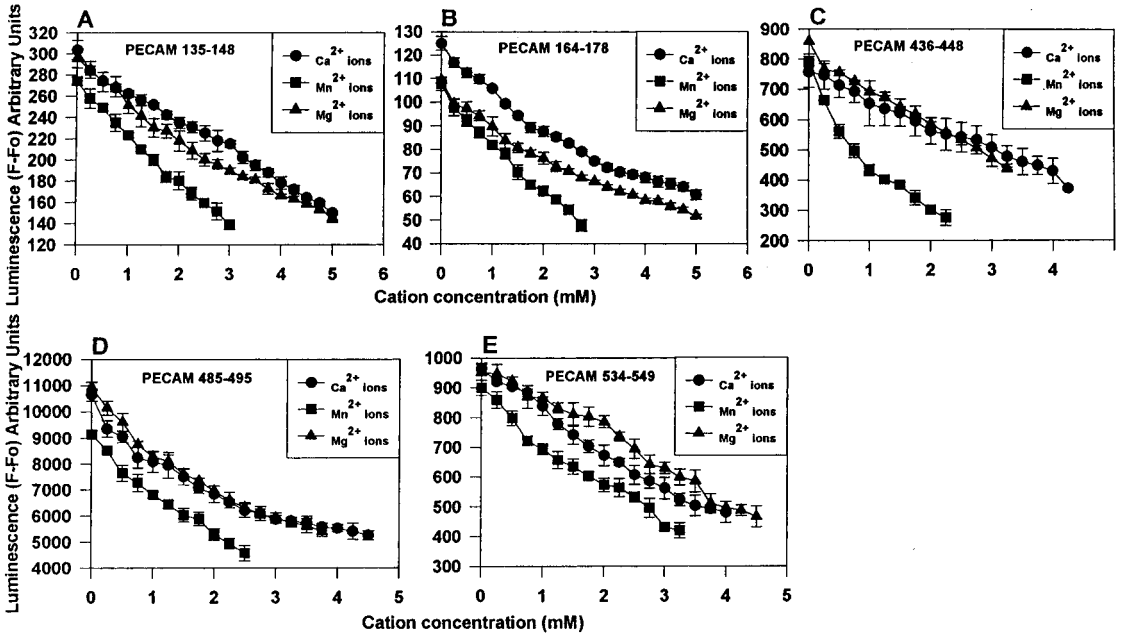

FIGURE 5: Displacement of Tb^{3+} from candidate PECAM (Y,W) peptides with divalent cations, Ca^{2+}, Mg^{2+}, and Mn^{2+}. Displacement curves for each of the candidate PECAM Ig-domain 2 (A, B), 5 (C), and 6 (D, E) (Y,W) peptides by sequential titration with each of the divalent cations as described under Experimental Procedures. Note that Tb^{3+} luminescence was reduced by the addition of each divalent cation in a dose-dependent manner for each candidate PECAM-1 (Y,W) peptide, demonstrating specificity of the interactions.

constants are comparable to those obtained for synthetic peptide loops for calmodulin and troponin C (Borin *et al.*, 1989; Kanellis *et al.*, 1983). These data suggest that PECAM-1 contains up to two metal binding domains as predicted by the equilibruim dialysis studies, although the one located in Ig-domain 6 may be functionally more important due to the high-affinity interactions of the two distinct Ig-domain 6 peptides for divalent cations. In addition, the cation binding sites demonstrate a broad specificity for all divalent cations, with Mn^{2+} having a higher affinity than either Ca^{2+} or Mg^{2+}. Similar findings have also been described for the integrin family of cell surface receptors (Gailit & Ruoslahti, 1988; Altieri, 1991; Elices *et al.*, 1991; Dransfield *et al.*, 1992; Kern *et al.*, 1993; Sanchez-Aparicio *et al.*, 1993).

Formation of Binary Complexes between Terbium and PECAM Ig-Domain 5 and 6 Peptides. Independent evidence that PECAM Ig-domain 5 and 6 peptides bind cations was obtained by ESI-MS. In initial studies, titration of Tb^{3+} with each PECAM peptide was performed to select the appropriate Tb^{3+} to peptide ratios to obtain optimal Tb^{3+} binding by ESI-MS (data not shown). As shown in the lower panel of Figure 6A, in the absence of terbium, the PECAM 436−448 (Y,W) Ig-domain 5 peptide had two major peaks at *m/z* 823 and *m/z* 1623 corresponding to charged states of +1 and +2. Incubation of this peptide with 50 μM Tb^{3+} resulted in the appearance of three novel peaks at *m/z* 890, *m/z* 968, and *m/z* 1238. The *m/z* 890 and *m/z* 968 peaks correspond to the attachment of one and two Tb^{3+} ions to the +2 charged peptide. The *m/z* 1238 peak was composed of a peptide dimer with three Tb^{3+} ions bound to the +3 charged peptide. These results provide direct physical evidence that PECAM 436−448 can complex with Tb^{3+} with involvement of three coordination sites. Similarly, in Figure 6B, the PECAM 485−495 (Y,W) Ig-domain 6 peptide showed one predominant *m/z* peak at 1325. This peak corresponds to a charged state of +1. Charge distributions in electrospray ionization mass spectroscopy are governed by many factors including the peptide sequence, conformation, solvent, and instrumental parameters. It is very common for singly charged ions to be of low abundance or even absent in peptide spectra. Incubation of this peptide with 50 μM Tb^{3+} resulted in the appearance of five novel peaks at *m/z* 741, *m/z* 819, *m/z* 1040, *m/z* 1480, and *m/z* 1559. Each of these peaks corresponded with the attachment of Tb^{3+} ions to different charge states of the peptide as indicated. Analysis of PECAM 534−549 (W) Ig-domain 6 peptide revealed a predominant peak at *m/z* 946 (Figure 6C). Addition of Tb^{3+} resulted in the attachment of three Tb^{3+} ions as shown by the appearance of *m/z* 1024, *m/z* 1103, and *m/z* 1416 peaks. From these results, we conclude that both PECAM Ig-domain 6 peptides can form complexes with Tb^{3+} involving a minimum of three cation coordination sites.

The complex formation observed between Tb^{3+} and PECAM Ig-domain 5 and 6 peptides appears to be specific, as no peptide−Tb^{3+} complexes were observed with control peptides derived from other regions of the PECAM-1 molecule. Two different PECAM 516−530 and 553−567 Ig-domain 6 peptides failed to bind Tb^{3+} ions. In addition, other control peptides included RGDW and RGEW also failed to bind Tb^{3+} ions (data not shown). Both control Ig-domain 6 peptides lacked candidate cation coordination Asp or Glu residues; however, short RGDW and RGDW peptides containing either an Asp or a Glu residue also failed to bind Tb^{3+} (data not shown), as previously described (D'Souza *et al.*, 1994).

The lower panels of Figures 6 show that dimers were not observed in the absence of terbium. (Those charge state assignments are readily confirmed by the spacing of the Na^+ adducts.) Dimerization appears to be enhanced in the presence of the Tb^{3+} ions, since the dimers are only observed in the metal ion containing solutions. It is clear that not all of the terbium binding arises from dimers by closely examining the peak spacings for the different charge states. For example, Figure 6A−C shows dimer coordinating to three terbiums in the 1200 (Figure 6A), 1000 (Figure 6B),

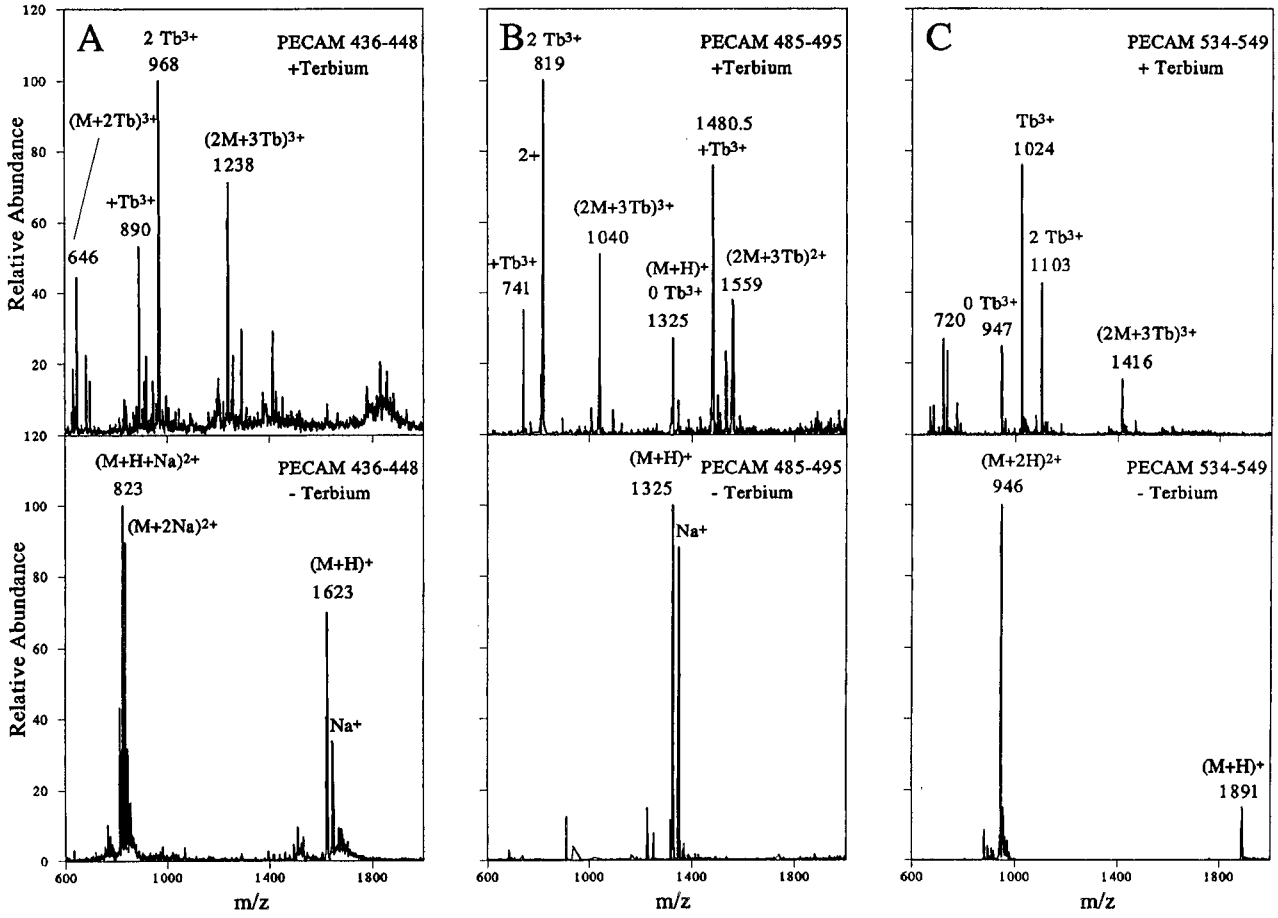

FIGURE 6: Formation of complexes between PECAM Ig-domain 5 and 6 (Y,W) peptides and terbium as observed by ESI-MS. Candidate PECAM Ig-domain 5 (436−448) (panel A) and 6 (485−495 and 534−549) (panels B and C) (Y,W) peptides (20 μM) were dissolved in distilled water and incubated overnight at 4 °C in the presence (upper panel) and absence (lower panel) of 50 μM $TbCl_3$. Samples were dried and rehydrated in 100% H_2O just prior to ESI-MS analysis as described under Experimental Procedures. Other control peptides included RGDW, RGEW, PECAM 516−530 (KPFYQMTSNATQAFW), and PECAM 553−567 (HASSVPRSKILTVV); all failed to bind Tb^{3+} (data not shown).

and 1400 (Figure 6C) *m/z* regions. The series of peaks from 800−1000 (Figure 6A), 700−900 (Figure 6B), and 900−1100 (Figure 6C) *m/z* have a spacing consistent with doubly charged ions. If they arose from a quadruply charged dimer instead, it could then bind only even numbers of terbiums, inconsistent with the previous data clearly showing three terbiums binding to the dimer. Hence, the peaks in the 800−1000 (Figure 6A), 700−900 (Figure 6B), and 900−1100 (Figure 6C) *m/z* regions are doubly charged. A second indication that terbium binding is not limited to dimers is provided by the upper panel of Figure 6A, where if it was asserted that only dimers were binding terbium, then dimers would be appearing in the 3+, 4+, and 6+ charge states, but not the 5+ charge state. Since electrospray ionization does not "skip" charge states, such an explanation cannot be correct.

Identification of Candidate Asp and Glu Residues Important for Coordinating Cation Binding in PECAM Ig-Domains 5 and 6. To identify critical residues involved in cation coordination, we substituted Ala residues in place of candidate Asp or Glu residues in PECAM Ig-domain 5 and 6 peptide sequences and monitored cation binding by Tb^{3+} luminescence spectroscopy (refer to Table 1 for peptide sequences). As shown in Figure 7, single Ala substitutions in potential cation binding sites for PECAM 436−448 (Y,W) (Ala_{443}, Ala_{444}, and Ala_{446}), PECAM 485−495 (Y,W) (Ala_{487}, Ala_{490}, Ala_{491}), and PECAM 534−549 (W) (Ala_{538}, Ala_{540}, and Ala_{542}) all resulted in reduction in Tb^{3+} luminescence. As shown in panel A of Figure 7, substitution of Ala for Asp at position 444 or Ala for Glu at position 443 resulted in a 2-fold reduction, while substitution of Ala for Glu at position 446 resulted in a moderate 3-fold reduction in Tb^{3+} luminescence, indicating that these modified peptides have lower affinity for Tb^{3+} than the wild-type PECAM 436−448 (Y,W). In contrast, substitution of Ala for Asp at position 439 resulted in only a minor reduction in Tb^{3+} luminescence. Binding studies with the PECAM 485−495 (Y,W) peptide showed that substitution of Ala for Glu at positions 487 and 490 resulted in a 2-fold reduction in Tb^{3+} luminescence, while substitution of Ala for Asp at position 491 resulted in a moderate 3-fold reduction in Tb^{3+} luminescence (panel B, Figure 7). When Ala was substituted for Glu residues at positions 538 or 540, a 2-fold reduction was observed, while substitution of Ala for Glu at position 542 in the PECAM 534−549 (W) peptide resulted in a 4-fold reduction in Tb^{3+} luminescence (panel C, Figure 7). The most prominent (5-fold) decrease in energy transfer was observed in peptides harboring double Ala substitutions, including PECAM 436−448 (Y,W) ($Ala_{433,444}$) and PECAM 485−495 (Y,W) ($Ala_{490,491}$) (data not shown), indicating that these modified peptides have a much lower affinity for Tb^{3+} and that these Asp and Glu residues mediate cation binding to PECAM-1. Direct Tb^{3+} binding to peptides harboring these Ala substitutions was also observed using ESI-MS, and

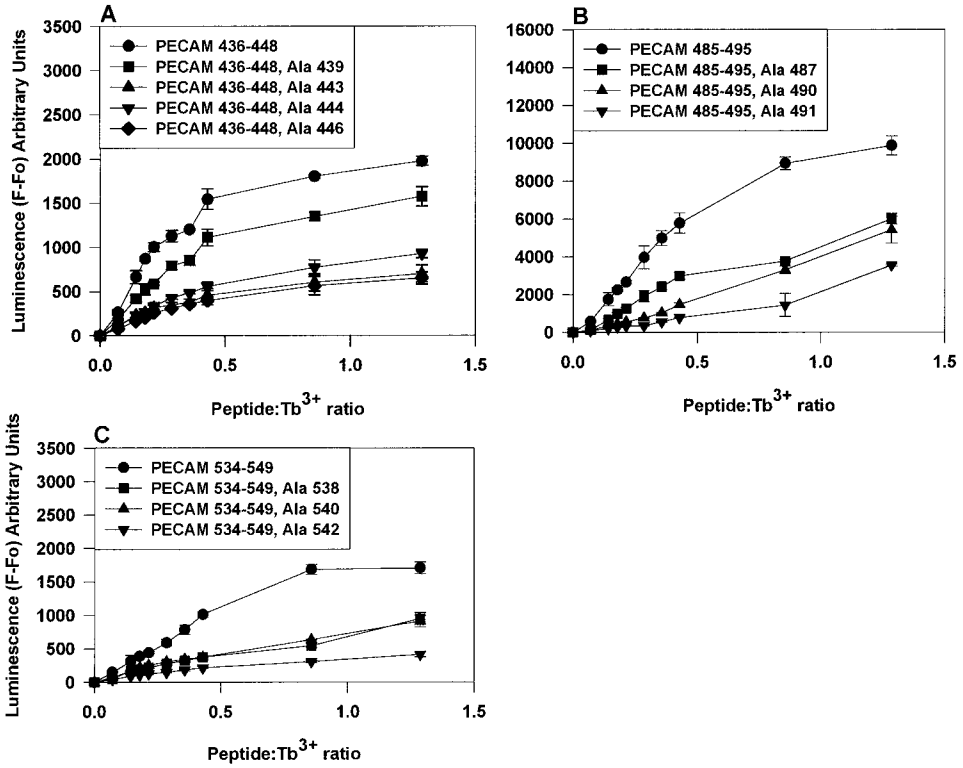

FIGURE 7: Metal binding properties of alanine-substituted cation coordination sites in PECAM Ig-domains 5 and 6. Titration curves of the interaction of Tb^{3+} with Ala-substituted synthetic peptides of candidate sequences in PECAM Ig-domains 5 (A) and 6 (B, C). The sequences of the three peptides examined are provided in detail in Table 1, and in each case include a modified wild-type PECAM sequence (Y,W) (●) and various Ala substitutions as indicated. Results are expressed as the mean ± standard deviation of three independent experiments. Tb^{3+} luminescence was excited at 285 nm and measured at 545 nm. Note that the Ala substitutions resulted in reduced Tb^{3+} luminescence of the PECAM Ig-domain 5 and 6 peptides.

each candidate cation coordination site resulted in loss of a peptide−Tb^{3+} complex (data not shown). Based on these results, we conclude that for Ig-domain 6, PECAM 534−549 (W) contains three cation coordination sites involving residues Glu_{538}, Glu_{540}, and Glu_{542} and PECAM 485−495 (Y,W) contains three cation coordination sites involving residues Glu_{487}, Glu_{490}, and Asp_{491}. Additionally, in Ig-domain 5, PECAM 436−448 (Y,W) also contains three cation coordination sites involving residues Asp_{443}, Asp_{444}, and Glu_{446}.

DISCUSSION

In this study, we have employed $^{45}CaCl_2$ binding studies, Tb^{3+} luminescence spectroscopy and ESI-MS to identify and characterize the interaction of metal ions with PECAM-1 and define unique cation binding domains using short, linear peptide sequences from the receptor. Our major findings are summarized as follows: First, PECAM-1 can directly interact with metal ions, demonstrated by 2.3 nmol of Ca^{2+}/nmol of srPECAM-1. This interaction can be mimicked by the calcium analog Tb^{3+} (Figures 1 and 2). Second, PECAM-1 contains high-affinity divalent cation binding sites involving Ig-domains 5 and 6 (Figure 4, Table 2). Third, the PECAM cation binding sites demonstrate broad specificity for all divalent cations with Mn^{2+} conferring a higher affinity than either Ca^{2+} or Mg^{2+} (Table 2).

Our study was initially prompted by the observation that PECAM-1 may have dual roles in both Ca^{2+}-independent homophilic and Ca^{2+}-dependent heterophilic cell interactions depending on the species and cell type examined (Albelda *et al*., 1991). This finding was somewhat unusual for a member of the Ig-gene superfamily, but has also been demonstrated with a neuron−glia cell adhesion molecule (Ng-CAM) (Grumet & Edelman, 1988). In this study, we have used several independent approaches, $^{45}CaCl_2$ binding, fluorescence energy transfer, and mass spectroscopy analysis, to provide clear evidence that PECAM-1 contains functional metal binding regions involving a high-affinity region (485−495 and 534−549) involving Ig-domain 6, which may be possibly linked to region 436−448 in Ig-domain 5. Examination of srPECAM-1 protein demonstrated an ability to directly bind $^{45}CaCl_2$ and compete for Tb^{3+} binding (Figures 1 and 2). Each of the candidate PECAM peptides could bind Tb^{3+} as assessed by fluorescence energy transfer (Figure 4). This interaction could be displaced by divalent cations, Ca^{2+}, Mg^{2+}, and Mn^{2+} ions, indicating their ability to bind to these metal binding regions in the PECAM-1 molecule (Figure 5). Confirmatory evidence of metal ion binding was shown by the formation of PECAM peptide−Tb^{3+} complexes using ESI-MS (Figure 6). Taken together, these data demonstrate that PECAM-1 contains functional metal binding regions localized to Ig-domains 5 and 6.

This study represents the first detailed report describing the identification and characterization of metal binding regions in a member of the Ig-gene superfamily. This is of particular interest as divalent cations play an important role in a variety of important biological functions, which is often accomplished through interactions with proteins. In cell-mediated adhesion, divalent cations are known to have multiple effects on ligand interactions by influencing ligand recognition specificity and regulation of ligand binding (Smith *et al*., 1994). The candidate PECAM cation binding

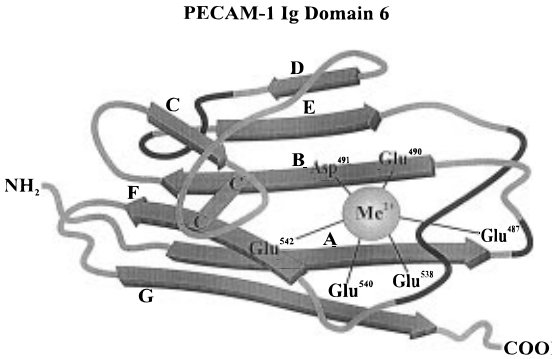

FIGURE 8: Hypothetical model of a high-affinity metal binding region located in PECAM Ig-domain 6. Two linear regions within Ig-domain 6, PECAM 485−495 and 534−549, are located close to each other in three-dimensional space, and are proposed to form a single divalent cation coordination region.

regions identified in this study contain clusters of acidic residues, but the spacing of these oxygenated residues and the lack of flanking α-helices do not strictly conform to conventional EF-hand motifs found in Ca^{2+} binding proteins such as calmodulin and platelet glycoprotein IIb or the recently described MIDAS domain (DXSXS) found in A domain superfamily members, which includes β subunits of integrins (Tuckwell *et al*., 1992; D'Souza *et al*., 1994; Lee *et al*., 1995). Homology alignment of EF-hand structures in calcium binding proteins has shown a degree of heterogeneity in their respective cation coordination sites, and many are described as loosely conforming to EF-hand motifs (Tuckwell *et al*., 1992; Cierniewski *et al*., 1994). Functional EF-hands conform to a consensus sequence, X-2-Y-4-Z-6-($^-$Y)-8-($^-$X)-10-11-($^-$Z), where the numbering of amino acids indicates the various positions within the cation binding loop. It can be noted that PECAM Ig-domain 6 534−549 peptide contains five appropriately spaced oxygenated residues in cation coordination positions 1 (X) (Glu), 3 (Y) (Glu), 5 (Z) (Glu), 7 ($^-$Y) (Tyr), and 12 ($^-$Z) (Asn) such as those found in Ca^{2+} binding EF-hand structures. Interestingly, this PECAM cation binding region is also highly conserved among various species including canine, rat, and murine (data not shown).

In order to conceptualize these metal binding regions in the PECAM-1 molecule, we superimposed the amino acid sequence of PECAM-1 onto the immunoglobin constant domain β-strands and loops. Computer-generated β-sheet analysis of PECAM-1's structure revealed that the PECAM 534−549 sequence was located between β-strands E and F and the PECAM 485−495 sequence was located between β-strands A and B in Ig-domain 6 (Figure 8). Modeling studies predict that the two PECAM Ig-domain 6 peptides are proximal to each other in three-dimensional space to form a single divalent cation coordination region. The precise relationship of the Ig-domain 5 site with the Ig-domain 6 regions awaits the solution of the crystal structure of PECAM-1.

Recent studies have suggested that Ig-domain 6 of PECAM-1 may be of functional importance in the regulation of PECAM-1 function. Specifically, a highly conserved region, 551−567, in the PECAM-1 molecule was shown to inhibit lymphocyte activation (Zehnder *et al*., 1995), and long-range propagation of the homophilic adhesive properties of Ig-domains 1 and 2 mediated by stimulation of Ig-domain 6 has been demonstrated (Sun, Q.-H., *et al*., 1996). It is also interesting that monoclonal antibodies which map to Ig-domains 2 and 6 both inhibited L-cell aggregation of a mixture of CD31-transfected and nontransfected cells (Albelda *et al*., 1992). We predict that the positioning of a high-affinity divalent cation binding region involving Ig-domain 6 immediately proximal to the cell surface may play an important role in the maintenance of the local conformation and stabilization of Ig-homology domains involved in downstream signaling events that emanate from PECAM-1 homophilic engagement.

In summary, the binding of divalent cations has been shown to be critical in supporting the adhesive properties of a number of cell surface receptors, including cadherins, integrins, and selectins (Takeichi, 1991; Ruoslahti, 1991; Yednock *et al*., 1987; Geng *et al*., 1991). In this study, we have demonstrated that PECAM-1 contains functional metal binding regions involving Ig-domains 5 and 6. Additional studies will help clarify the role of divalent cations in stabilizing the adhesive or signaling properties of PECAM-1, and should provide an insight into the structural basis for PECAM-1-mediated cellular interactions.

ACKNOWLEDGMENT

We are grateful to Lorie Miller for her assistance in the Biophysics Core Laboratory, and to Drs. Richard Aster and Peter Sims for helpful advice.

REFERENCES

Albelda, S. M., Oliver, P., Romer, L., & Buck, C. A. (1990) *J. Cell Biol. 110*, 1227−1237.
Albelda, S. M., Muller, W. A., Buck, C. A., & Newman, P. J. (1991) *J. Cell Biol. 114*, 1059−1068.
Albelda, S. M., DeLisser, H. M., Yan, H. C., Muller, W. A., Buck, C. A., & Newman, P. J. (1992) *Clin. Res. 40*, 355a.
Altieri, D. C. (1991) *J. Immunol. 147*, 1891−1898.
Ayalon, O., Sabanai, H., Lampugnani, M.-G., Dejana, E., & Geiger, B. (1994) *J. Cell Biol. 126*, 247−258.
Baldwin, H. S., Shen, H. M., Chung, A., Mickanin, C., Trask, T., Yan, H., DeLisser, H. M., Albelda, S. M., Kirschbaum, N., Newman, P. J., & Buck, C. A. (1994) *Development 120*, 2539−2553.
Bogen, S., Pak, J., Garifallou, M., Deng, X., & Muller, W. A. (1994) *J. Exp. Med. 179*, 1059−1064.
Borin, G., Ruzza, P., Rossi, M., Calderan, A., Marchiori, F., & Peggion, E. (1989) *Biopolymers 28*, 353−369.
Buckley, C. D., Doyonnas, R., Newton, J. P., Blystone, S. D., Brown, E. J., Watt, S. M., & Simmons, D. L. (1996) *J. Cell Sci. 109*, 437−445.
Cierniewski, C. S., Haas, T. A., Smith, J. W., & Plow, E. F. (1994) *Biochemistry 33*, 12238−12246.
Cunningham, B. A., Hemperly, J. J., Murray, B. A., Prediger, E. A., Brackenbury, R., & Edelman, G. M. (1987) *Science 236*, 799−806.
DeLisser, H. M., Yan, C. Y., Newman, P. J., Muller, W. A., Buck, C. A., & Albelda, S. M. (1993) *J. Biol. Chem. 268*, 16037−16046.
Dransfield, I., Cabanas, E., Craig, A., & Hogg, N. (1992) *J. Cell Biol. 116*, 219−226.
D'Souza, S. E., Haas, T. A., Piotrowicz, R. S., Byers-Ward, V., McGrath, D. E., Soule, H. R., Cierniewski, C., Plow, E. F., & Smith, J. W. (1994) *Cell 79*, 659−667.
Elices, M. J., Urry, L. A., & Hemler, M. E. (1991) *J. Cell Biol. 112*, 169−181.
Fawcett, J., Buckley, C., Holness, C. L., Bird, I. N., Spragg, J. H., Saunders, J., Harris, A., & Simmons, D. L. (1995) *J. Cell Biol. 128*, 1229−1241.
Gailit, J., & Ruoslahti, E. (1988) *J. Biol. Chem. 263*, 12927−12932.
Gariepy, J., Kay, L. E., Kuntz, I. D., Sykes, B. D., & Hodges, R. S. (1985) *Biochemistry 24*, 544−550.

Geng, J.-G., Moore, K. L., Johnson, A. E., & McEver, R. P. (1991) *J. Biol. Chem. 266*, 22313−22318.
Goldberger, A., Middleton, K. A., Oliver, J. A., Paddock, C., Yan, H.-C., DeLisser, H. M., Albelda, S. M., & Newman, P. J. (1994) *J. Biol. Chem. 269*, 17183−17191.
Grumet, M., & Edelman, G. M. (1988) *J. Cell Biol. 106*, 487−503.
Hynes, R. O. (1992) *Cell 69*, 11−25.
Jackson, D. E., Poncz, M., Holyst, M. T., & Newman, P. J. (1996) *Eur. J. Biochem. 240*, 280−287.
Jackson, D. E., Ward, C. M., Wang, R., & Newman, P. J. (1997) *J. Biol. Chem. 272*, 6986−6993.
Kern, A., Eble, J., Golbik, R., & Kuhn, K. (1993) *Eur. J. Biochem. 215*, 151−159.
Lee, J.-O., Rieu, P., Arnaout, M. A., & Liddington, R. (1995) *Cell 80*, 631−638.
Marsden, B. J., Hodges, R. S., & Sykes, B. D. (1989) *Biochemistry 28*, 8839−8847.
Mauro, V. P., Krushel, L. A., Cunningham, B. A., & Edelman, G. M. (1992) *J. Cell Biol. 119*, 191−202.
Muller, W. A., Ratti, C. M., McDonnell, S. L., & Cohn, Z. A. (1989) *J. Exp. Med. 170*, 399−414.
Muller, W. A., Weigl, S. A., Deng, X., & Phillips, D. M. (1993) *J. Exp. Med. 178*, 449−460.
Newman, P. J. (1994) *Ann. N.Y. Acad. Sci.* 165−174.
Newman, P. J., & Albelda, S. M. (1992) *Nouv. Rev. Fr. Hematol. 34*, 9−13.
Newman, P. J., Berndt, M. C., Gorski, J., White, G. C., Lyman, S., Paddock, C., & Muller, W. A. (1990) *Science 247*, 1219−1222.
Novotny, J., & Auffray, C. (1984) *Nucleic Acids Res. 12*, 243−255.
Piali, L., Hammel, P., Uherek, C., Gisler, R. H., Dunon, D., & Imhof, B. A. (1995) *J. Cell Biol. 130*, 451−460.
Rao, Y., Wu, X., Gariepy, J., Rutishauser, U., & Siu, C. (1992) *J. Cell Biol. 118*, 937−949.
Rose, G. D., & Roy, S. (1980) *Proc. Natl. Acad. Sci. U.S.A. 77*, 4643−4647.
Ruoslahti, E. (1991) *J. Clin. Invest. 87*, 1−5.
Sanchez-Aparicio, P., Ferreira, O. C., Jr., & Garcia-Pardo, A. (1993) *J. Immunol. 150*, 3506−3514.
Smith, J. W., Piotrowicz, R. S., & Mathis, D. (1994) *J. Biol. Chem. 269*, 960−967.
Springer, T. A. (1990) *Nature 346*, 425−434.
Sun, J., Williams, J., Yan, H. C., Amin, K. M., Albelda, S. M., & DeLisser, L. M. (1996) *J. Biol. Chem. 271*, 18561−18170.
Sun, Q.-H., DeLisser, H. M., Zukowski, M. M., Paddock, C., Albelda, S. M., & Newman, P. J. (1996) *J. Biol. Chem. 271*, 11090−11098.
Takeichi, M. (1991) *Science 251*, 1451−1455.
Tanaka, Y., Albelda, S. M., Horgan, K. J., van Seventer, G. A., Shimizu, Y., Newman, W., Hallam, J., Newman, P. J., Buck, C. A., & Shaw, S. (1992) *J. Exp. Med. 176*, 245−253.
Tuckwell, D. S., Brass, A., & Humphries, M. J. (1992) *Biochem. J. 285*, 325−331.
Vaporciyan, A. A., DeLisser, H. M., Yan, H., Mendiguren II, Thom, S. R., Jones, M. L., Ward, P. A., & Albelda, S. M. (1993) *Science 262*, 1580−1582.
Williams, A. F., & Barclay, A. N. (1988) *Annu. Rev. Immunol. 6*, 381−405.
Yan, H., Pilewski, J. M., Zhang, Q., DeLisser, H. M., Romer, L., & Albelda, S. M. (1995) *Cell Adhes. Commun. 3*, 45−66.
Yednock, T. A., Stoolman, L. M., & Rosen, S. D. (1987) *J. Cell Biol. 104*, 713−723.

BI970084X